

Symmetry Energy from Experiment, Theory and Observation

J. M. Lattimer

Department of Physics & Astronomy



The Modern Physics of Compact Stars
and Relativistic Gravity 2023

Yerevan, Armenia, Sep. 12-16, 2023

Acknowledgements

Funding Support:

DOE - Nuclear Physics

DOE - Toward Exascale Astrophysics of Mergers and Supernovae (TEAMS)

NASA - Neutron Star Interior Composition ExploreR (NICER)

NSF - Neutrinos, Nuclear Astrophysics and Symmetries (PFC - N3AS)

DOE - Nuclear Physics from Multi-Messenger Mergers (NP3M)

Recent Collaborators:

Duncan Brown & Soumi De (Syracuse), Christian Drischler, Madappa Prakash & Tianqi Zhao (Ohio), Sophia Han (TDLI), Evgeni Kolomeitsev (Matej Bei, Slovakia), Akira Ohnishi (YITP, Kyoto), Sanjay Reddy (INT), Achim Schwenk (Darmstadt), Andrew Steiner (Tennessee) & Ingo Tews (LANL)

Nuclear Symmetry Energy and Pressure

The symmetry energy is the difference between the energies of pure neutron matter ($x = 0$) and symmetric ($x = 1/2$) nuclear matter:

$$S_2(n) = E(n, x = 0) - E(n, x = 1/2).$$

The quadratic term in an expansion of neutron excess $1 - 2x$ dominates:

$$E(n, x) = E(n, 1/2) + (1 - 2x)^2 S_2(n) + \dots$$

Expanding S_2 about saturation n_s :

$$S_2(n) = J + \frac{L}{3} \frac{n - n_s}{n_s} + \dots$$

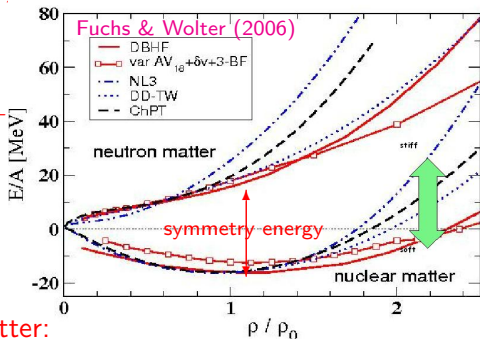
$$J \simeq 31 \text{ MeV}, \quad L \simeq 50 \text{ MeV}$$

Extrapolated to pure neutron matter:

$$E_N = E(n_s, 0) \approx J + E(n_s, 1/2) \equiv J - B, \quad P_N = P(n_s, 0) = Ln_s/3$$

Neutron star matter (beta equilibrium) is nearly neutron matter:

$$\frac{\partial(E + E_e)}{\partial x} = 0, \quad P_{NSM}(n_s) \simeq \frac{Ln_s}{3} \left[1 - \left(\frac{4J}{\hbar c} \right)^3 \frac{4 - 3J/L}{3\pi^2 n_s} \right]$$

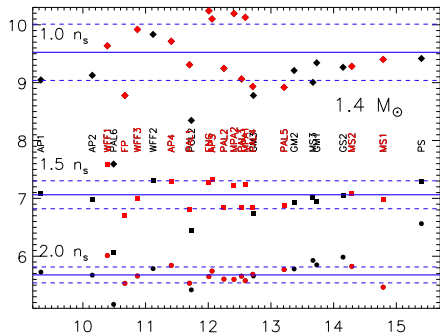
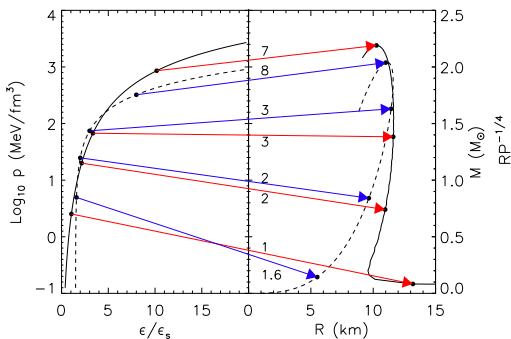


Why is the Symmetry Energy Important?

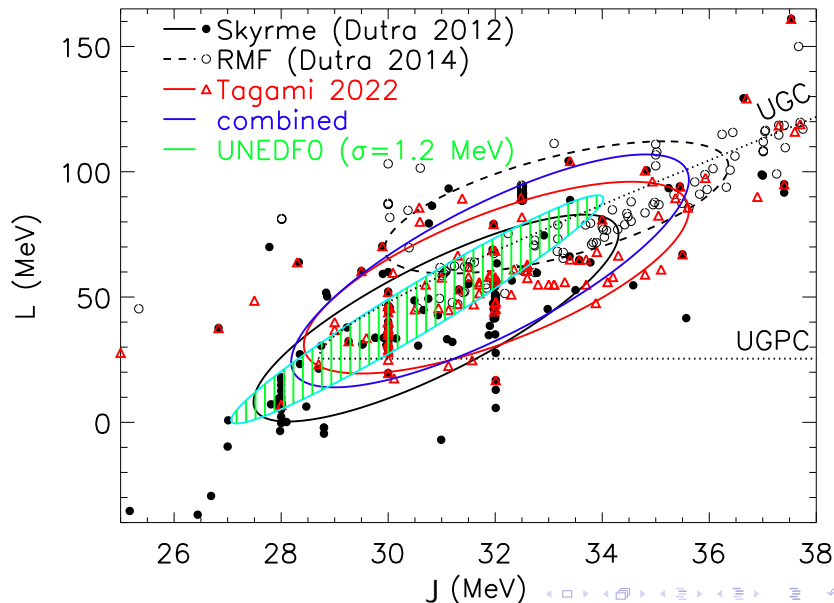
The equation of state in a neutron star depends strongly on the density dependence of the symmetry energy ($u = n_B/n_s$):

$$P_{NSM}(u) \simeq n_s u^2 \left[\frac{L}{3} + \frac{K_N}{9}(u - 1) + \frac{Q_N}{54}(u - 1)^2 + \dots \right].$$

A strong correlation exists between radii and P_{NSM} near n_s :
 $R_{1.4} \sim P_{NSM}(n_B)^{1/4}$.



Fitting Nuclear Binding Energies



Meaning of $J - L$ Correlations

The slope dL/dJ is an indicator of the most sensitive density u_s for the measurement of the symmetry energy $S(u)$.

If the correlation line goes through (J, L) , a change dJ can be compensated by a change dL .

$$\frac{dJ}{dL} = - \left(\frac{\partial S(u_s)}{\partial L} \right)_J / \left(\frac{\partial S(u_s)}{\partial J} \right)_L.$$

Example: $S(u) = S_K u^{2/3} + S_V u^\gamma$, $S_K \simeq 12.5$ MeV
 $J = S_K + S_V$, $L = 2S_K + 3\gamma S_V = S_K(2 - 3\gamma) + 3\gamma J$

$$\frac{dJ}{dL} = -\frac{\ln u_s}{3}, \quad u_s = \exp\left(-3\frac{dJ}{dL}\right).$$

For binding energies, $dL/dJ \simeq 11$, $u_s \simeq 0.76$.

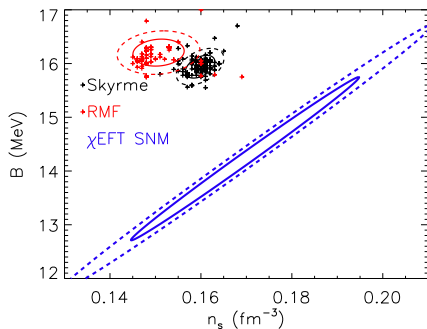
Saturation Properties of Nuclear Interactions

Empirical Saturation Window

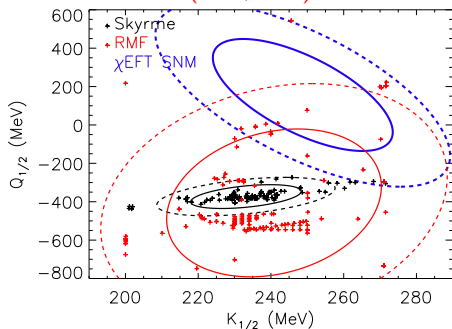
$$B = 16.06 \pm 0.20 \text{ MeV}$$

$$n_s = 0.1558 \pm 0.0054 \text{ fm}^{-3}$$

$$K_{1/2} = 236.5 \pm 15.4 \text{ MeV}$$

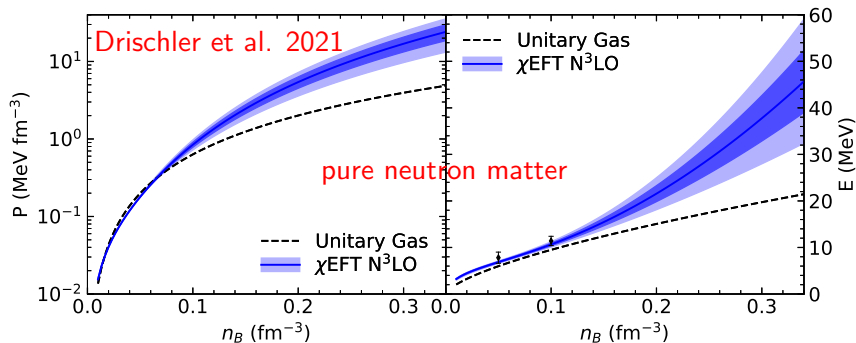


Data from Dutra (2012, 2014)



Theoretical Neutron Matter Studies

Recently developed chiral effective field theory allows a systematic expansion of nuclear forces at low energies based on the symmetries of quantum chromodynamics. It exploits the gap between the pion mass (the pseudo-Goldstone boson of chiral symmetry-breaking) and the energy scale of short-range nuclear interactions established from experimental phase shifts. It provides the only known consistent framework for estimating energy uncertainties.



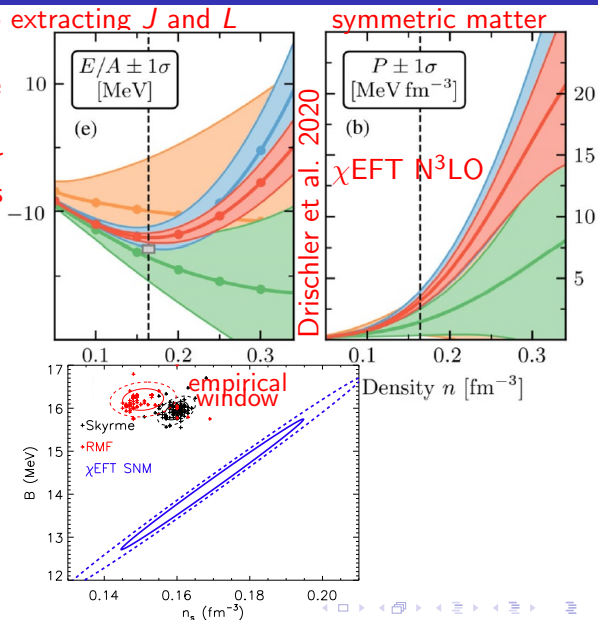
Symmetry Parameters From Chiral EFT

Two approaches to extracting J and L

1. Take the difference between pure neutron and symmetric matter energies and pressures at the calculated saturation density.

2. Use pure neutron matter energy and pressure with the empirical saturation window from nuclear mass fits.

$$J = E_N(n_s) + B,$$
$$L = 3P_N(n_s)/n_s.$$



Symmetry Parameters From Neutron Matter

Pure neutron matter calculations are more reliable than symmetric matter calculations.

Symmetric matter emerges from a delicate cancellation sensitive to short- and intermediate-range three-body interactions at N²LO that are Pauli-blocked in pure neutron matter.

N³LO symmetric matter calculations don't saturate within empirical ranges for n_s and B ,

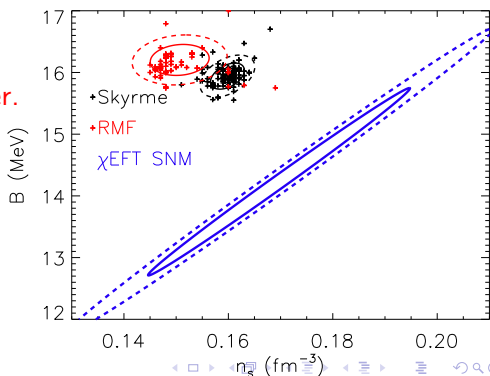
and introduce spurious correlations in symmetric matter.

We infer symmetry parameters from $E_N(n_s)$ and $P_N(n_s)$ using

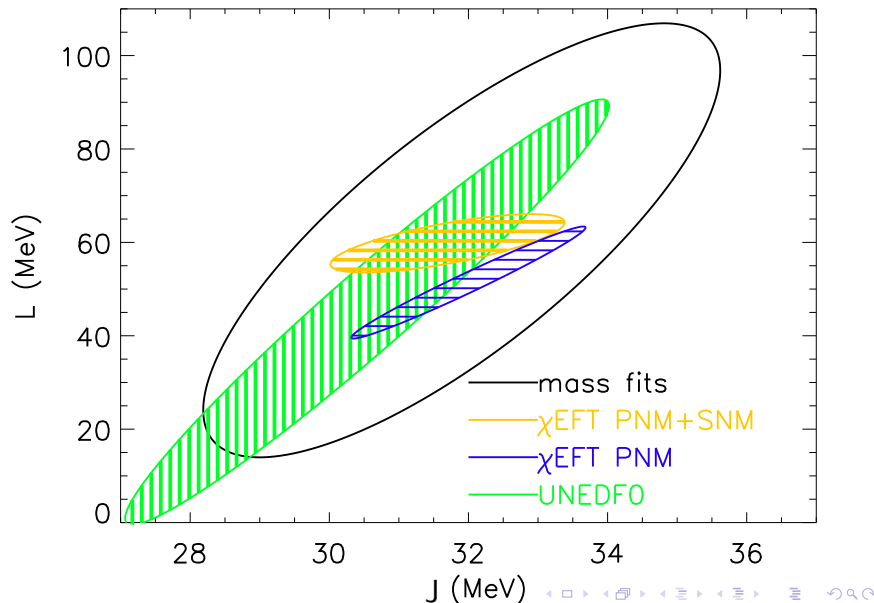
$$J = E_N(n_s) + B$$

$$L = 3P_N(n_s)/n_s$$

and include uncertainties in E_N , P_N , n_s and B .



Correlations From Chiral EFT



Bounds From The Unitary Gas Conjecture

The Conjecture (UGC):

Neutron matter energy always larger than unitary gas energy.

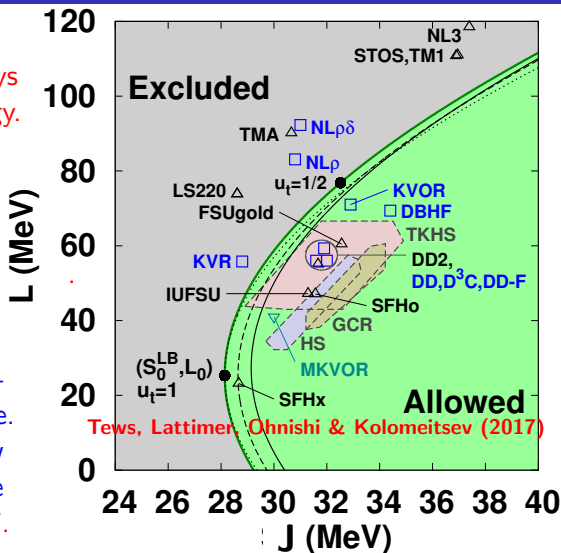
$E_{UG} = \xi_0(3/5)E_F$, or

$$E_{UG} \simeq 12.6 \left(\frac{n}{n_s} \right)^{2/3} \text{ MeV.}$$

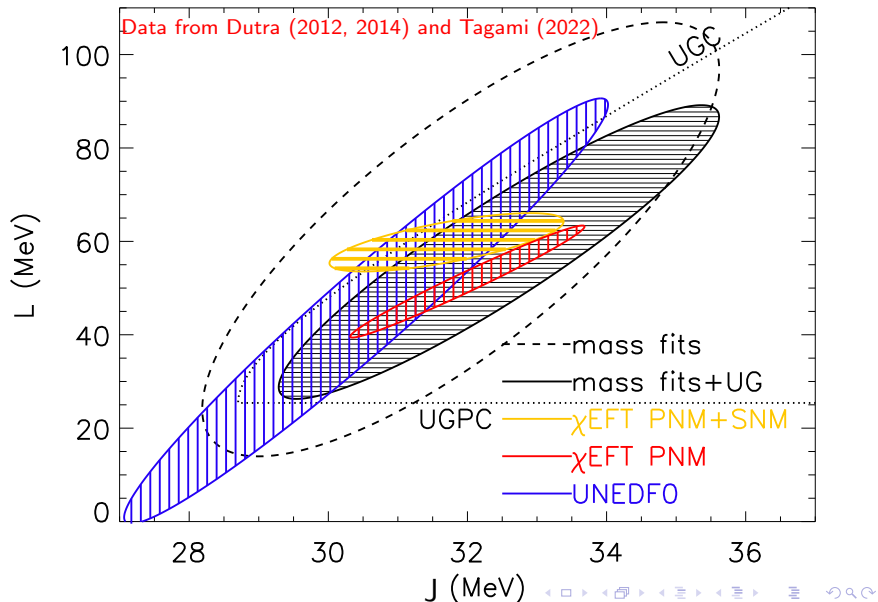
The unitary gas consists of fermions interacting via a pairwise short-range s-wave interaction with infinite scattering length and zero range. Cold atom experiments show a universal behavior with the Bertsch parameter $\xi_0 \simeq 0.37$.

For $n \geq n_s$, one also observes $P_N > P_{UG}$ (UGPC).

$J \geq 28.6 \text{ MeV}$; $L \geq 25.3 \text{ MeV}$; $P_N(n_s) \geq 1.35 \text{ MeV fm}^{-3}$; $R_{1.4} \geq 9.7 \text{ km}$.



Applying Unitary Gas Constraints



Neutron Skin Thickness

The difference between the mean neutron and proton radii in the liquid droplet model is

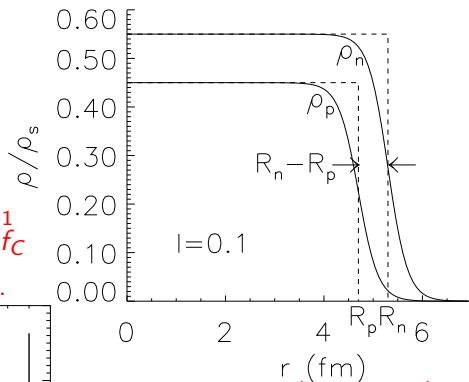
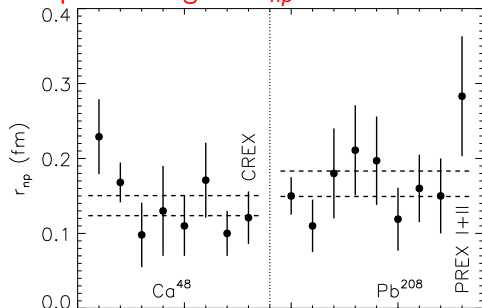
$$t_{np} = R_n - R_p.$$

The mean square difference is

$$r_{np}^2 = \langle R_n \rangle^2 - \langle R_p \rangle^2.$$

$$r_{np} = \sqrt{\frac{32r_0}{5} \frac{S_s}{3J} \left[1 + S_s A^{-1/3} / J \right]^{-1}} f_C$$

Implies strong $L - r_{np}$ correlation.



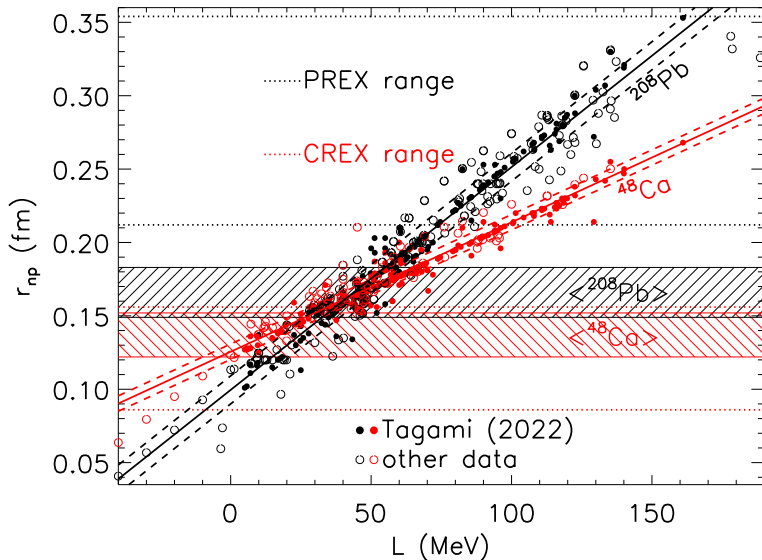
$$f_C = 1 - \frac{3Ze^2}{140IS_s r_0} \left(1 + \frac{10S_s}{3JA^{1/3}} \right)$$

For ^{208}Pb : $r_{np} \simeq 0.13$ fm

$$\frac{\Delta(S_s/J)}{\Delta J} \simeq -0.020$$

$$\frac{\Delta L}{\Delta J} = \frac{\Delta(S_s/J)}{\Delta J} \frac{1}{0.0234} \simeq -0.84$$

Calculated $L - r_{np}$ Correlations



Implied L Values

Historical experimental weighted average ^{208}Pb

$$r_{np}^{208} = 0.166 \pm 0.017 \text{ fm, implying } L = 45 \pm 13 \text{ MeV.}$$

Historical experimental weighted average ^{48}Ca

$$r_{np}^{48} = 0.137 \pm 0.015 \text{ fm, implying } L = 14 \pm 21 \text{ MeV.}$$

$$\text{Combined } L = 36 \pm 11 \text{ MeV.}$$

Parity-violating electron scattering measurements at JLab:

PREX I+II ^{208}Pb (Adhikari et al. 2021):

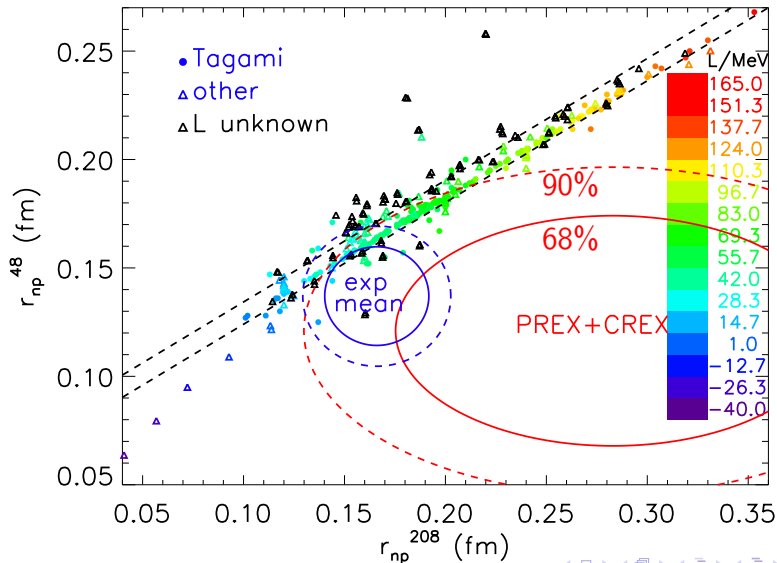
$$r_{np}^{208} = 0.283 \pm 0.071 \text{ fm, implying } L = 119 \pm 46 \text{ MeV.}$$

CREX ^{48}Ca (Adhikari et al. 2022):

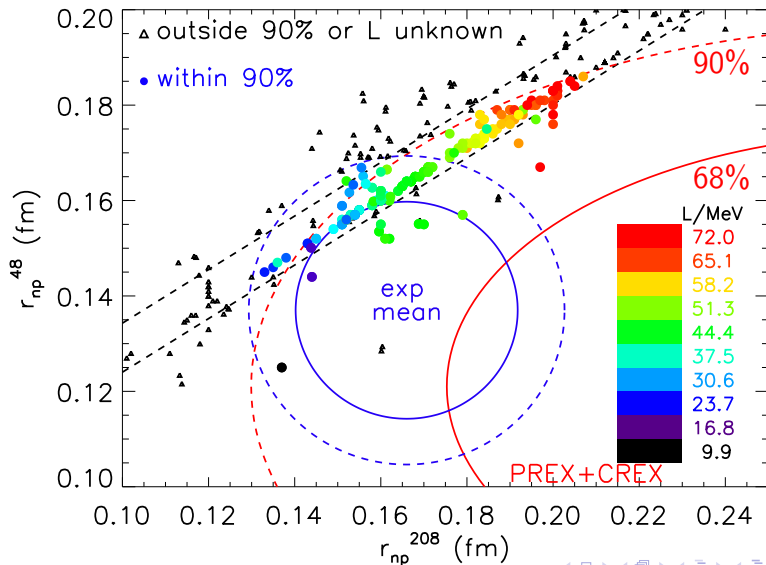
$$r_{np}^{48} = 0.121 \pm 0.035 \text{ fm, implying } L = -5 \pm 42 \text{ MeV.}$$

$$\text{Combined } L = 51 \pm 31 \text{ MeV.}$$

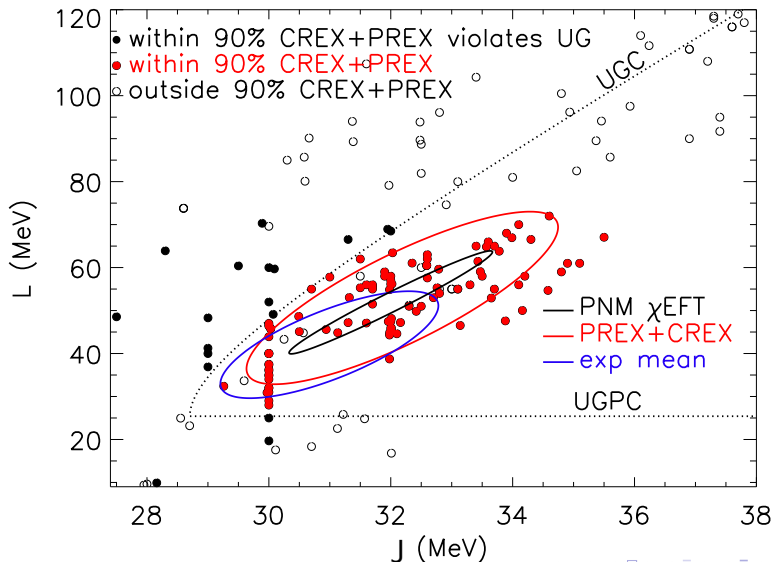
$r_{np}^{208} - r_{np}^{48}$ Linear Correlation



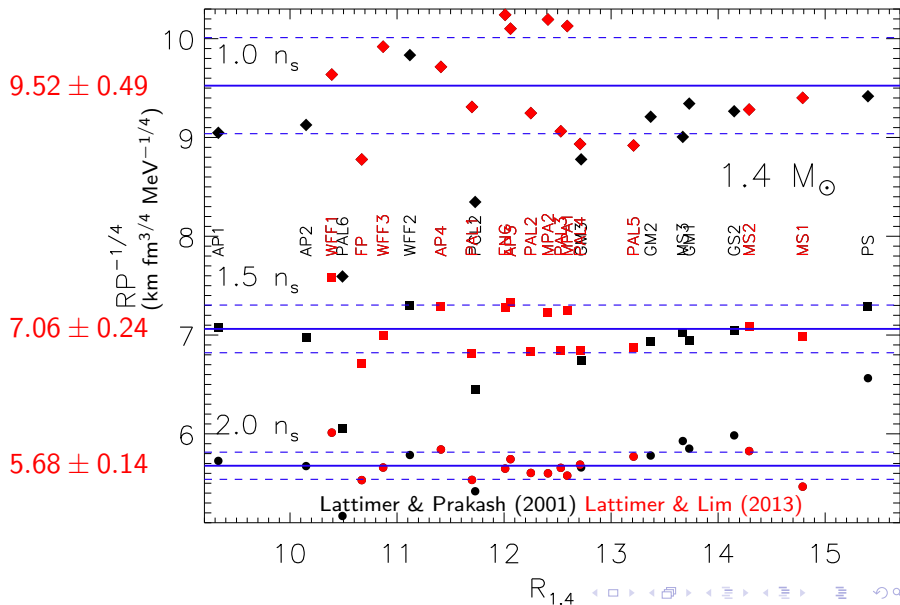
Detail



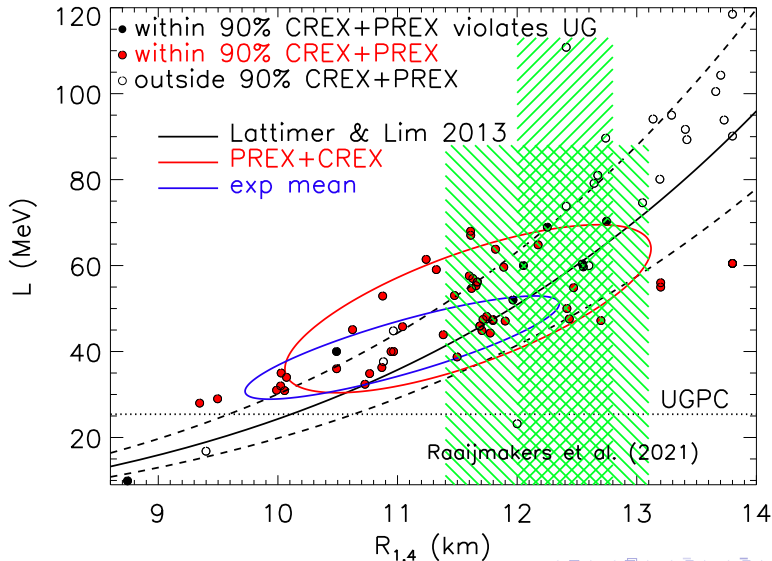
Implied $J - L$



The Radius – Pressure Correlation



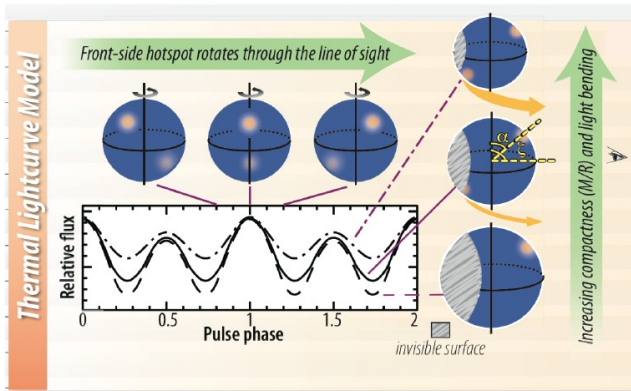
Implied $R_{1.4} - L$



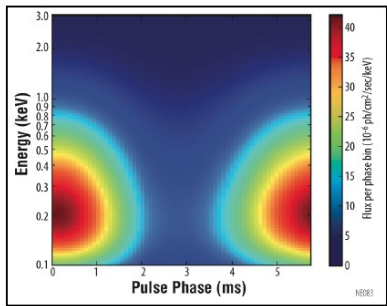
Science Measurements



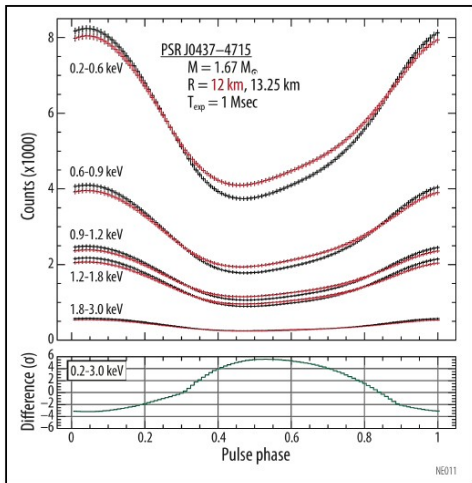
Reveal stellar structure through lightcurve modeling, long-term timing, and pulsation searches



Lightcurve modeling constrains the compactness (M/R) and viewing geometry of a non-accreting millisecond pulsar through the depth of modulation and harmonic content of emission from rotating hot-spots, thanks to gravitational light-bending...

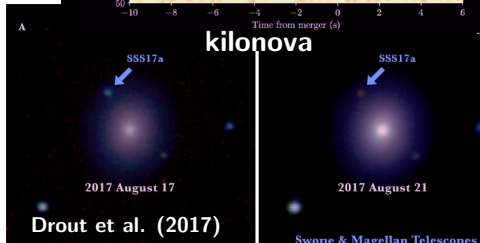
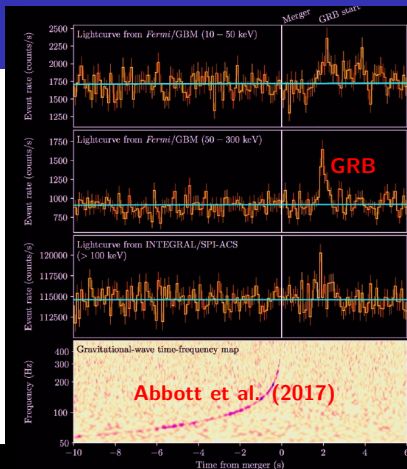


... while phase-resolved spectroscopy promises a direct constraint of radius R .



GW170817

- ▶ LVC detected a signal consistent with a BNS merger, followed 1.7 s later by a weak gamma-ray burst.
- ▶ $\simeq 10100$ orbits observed over 317 s.
- ▶ $\mathcal{M} = 1.186 \pm 0.001 M_{\odot}$
- ▶ $M_{T,\min} = 2^{6/5} \mathcal{M} = 2.725 M_{\odot}$
- ▶ $E_{\text{GW}} > 0.025 M_{\odot} c^2$
- ▶ $D_L = 40_{-14}^{+8}$ Mpc
- ▶ $75 < \tilde{\Lambda} < 560$ (90%)
- ▶ $M_{\text{ejecta}} \sim 0.06 \pm 0.02 M_{\odot}$
- ▶ Blue ejected mass: $\sim 0.01 M_{\odot}$
- ▶ Red ejected mass: $\sim 0.05 M_{\odot}$
- ▶ Probable r-process production
- ▶ Ejecta + GRB: $M_{\text{max}} \lesssim 2.22 M_{\odot}$



Tidal Deformability

The tidal deformability λ is the ratio of the induced dipole moment Q_{ij} to the external tidal field E_{ij} , $Q_{ij} \equiv -\lambda E_{ij}$.

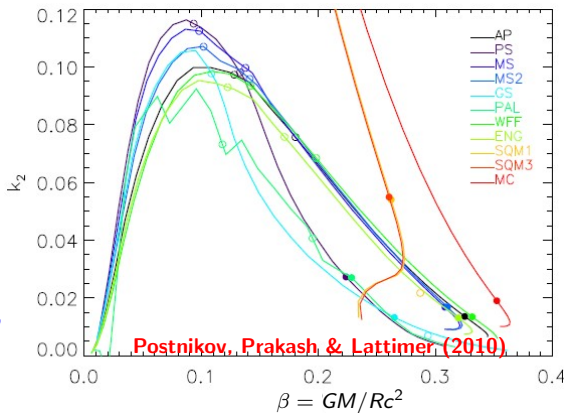
Use $\beta = GM/Rc^2$ and

$$\Lambda = \frac{\lambda c^{10}}{G^4 M^5} \equiv \frac{2}{3} k_2 \beta^{-5}.$$

$k_2 \propto 1/\beta$ is the dimensionless Love number, so $\Lambda \simeq a\beta^{-6}$.
For $1 < M/M_\odot < 1.6$,
 $a = 0.0093 \pm 0.0007$.

For a neutron star binary,
the mass-weighted $\tilde{\Lambda}$ is
the relevant observable:

$$\tilde{\Lambda} = \frac{16(1+12q)\Lambda_1 + (12+q)q^4\Lambda_2}{13(1+q)^5},$$



$$q = M_2/M_1 \leq 1$$

Binary Deformability and the Radius

$$\tilde{\Lambda} = \frac{16(1+12q)\Lambda_1 + q^4(12+q)\Lambda_2}{13(1+q)^5} \simeq \frac{16a}{13} \left(\frac{R_{1.4}c^2}{GM} \right)^6 \frac{q^{8/5}(12-11q+12q^2)}{(1+q)^{26/5}}.$$

This is very insensitive to q for $q > 0.5$, so

$$\tilde{\Lambda} \simeq a' \left(\frac{R_{1.4}c}{GM} \right)^6.$$

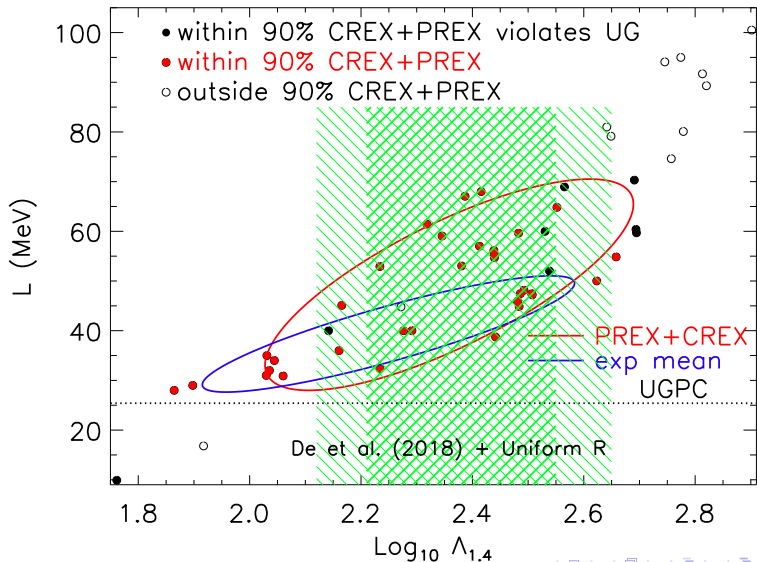
For $\mathcal{M} = (1.2 \pm 0.2) M_\odot$, $a' = 0.0035 \pm 0.0006$,

$$R_{1.4} = (11.5 \pm 0.3) \frac{\mathcal{M}}{M_\odot} \left(\frac{\tilde{\Lambda}}{800} \right)^{1/6} \text{ km.}$$

For GW170817, $\mathcal{M} = 1.186 M_\odot$, $a' = 0.00375 \pm 0.00025$,

$$R_{1.4} = (13.4 \pm 0.1) \left(\frac{\tilde{\Lambda}}{800} \right)^{1/6} \text{ km.}$$

Implied $\Lambda_{1.4} - L$



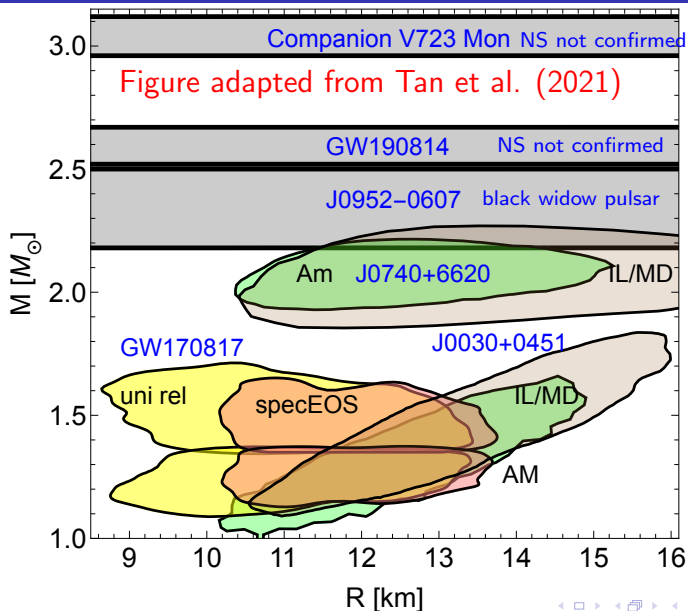
HESS J1731-347

- ▶ Doroshenko et al. quote $M = 0.77_{-0.17}^{+0.20} M_{\odot}$, $R = 10.4_{-0.78}^{+0.86}$ km, $D = 2.5 \pm 0.3$ km.
- ▶ Source is buried in a dust shell of estimated $2M_{\odot}$ with uncertain effects on atmospheric emission modeling.
- ▶ And corrected Gaia parallax indicates $D = 2.63_{-0.24}^{+0.35}$ kpc, and M and R inferences are both proportional to D .
- ▶ Single-temperature C atmosphere model gives $M = 0.83_{-0.13}^{+0.17} M_{\odot}$, $R = 11.25_{-0.37}^{+0.53}$ km, $D = 2.89_{-0.16}^{+0.20}$ kpc.
- ▶ Source flux variations have 10% upper limit, but if due to nonuniform surface T , M and R are underestimated.

Let $T_2 = aT_1$ with $a \sim 1.3$ and flux variation $f \sim 0.1$.

$$R^2 T^4 = R_1^2 T_1^4 + R_2^2 T_2^4 = R_1^2 T_1^4 / f$$
$$R^2 = R_2^2 \left[\frac{1 + f(a^4 - 1)}{1 - f} \right] \sim 1.32 R_2^2$$

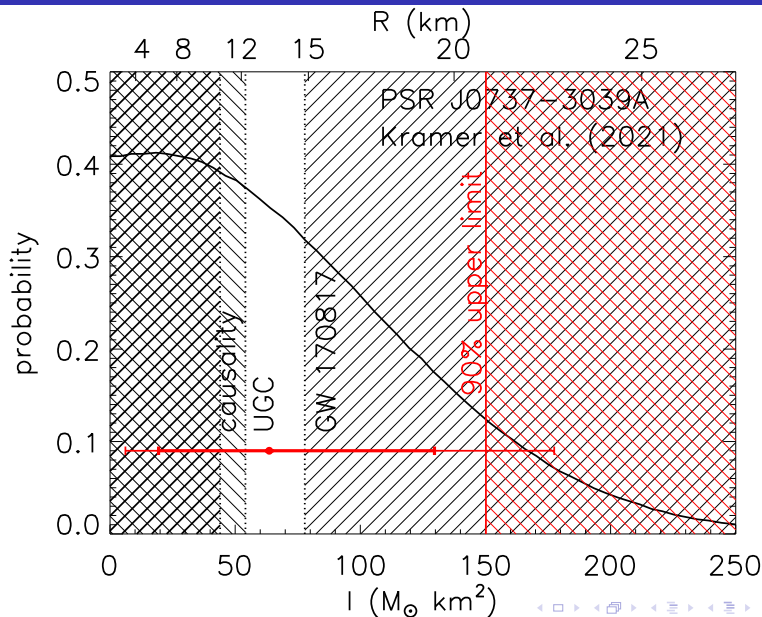
Summary of Astrophysical Observations



Moment of Inertia

- ▶ Spin-orbit coupling is of same magnitude as post-post-Newtonian effects (Barker & O'Connell 1975, Damour & Schaeffer 1988).
- ▶ Precession alters orbital inclination angle (observable if system is face-on) and periastron advance (observable if system is edge-on).
- ▶ More EOS sensitive than R : $I \propto MR^2$.
- ▶ Detection requires system to be extremely relativistic.
- ▶ Double pulsar PSR J0737-3037 ($P_b = 0.102$ d) is an edge-on candidate; $M_A = 1.338185 \pm 0.000004 M_\odot$.
- ▶ More relativistic systems have been found: PSR J1757-1854 ($M_A = 1.3412 \pm 0.0004 M_\odot$, $P_b = 0.164$ d) and J1946+2052 ($M_A < 1.31 M_\odot$, $P_b = 0.078$ d).
- ▶ Accurate (10%) I measurements expected by 2030 for both PSR J0737-3037 and J1757-1854.

Recent Moment of Inertia Measurement



S190426c: First Black Hole-Neutron Star Merger?

Information from LVC indicated a marginal case, with 58% chance of being 'terrestrial anomaly'.

Assuming it is cosmic in origin, GCN circular 24411 stated $p_{\text{BHNS}} = 0.60$, $p_{\text{gap}} = 0.35$, $p_{\text{BNS}} = 0.15$, $p_{\text{BBH}} < 0.01$, $p_{\text{HasNS}} > 0.99$ and $p_{\text{rem}} = 0.72$.

LVC defined BNS if both $M_{1,2} \leq 3M_{\odot}$, BH if both $M_{1,2} \geq 5M_{\odot}$ and gap if either mass satisfied $3M_{\odot} < M < 5M_{\odot}$.

LVC won't immediately release the chirp mass \mathcal{M} (even though it's known precisely), the mass ratio $q = M_1/M_2 > 1$ (and therefore M_1 and M_2 , known much less precisely), and the spin parameter χ if one component is a BH.

But it is still possible to recover \mathcal{M} , M_1 , M_2 and χ in cases where p_{BHNS} , p_{gap} , p_{BNS} and/or p_{rem} are nonzero.

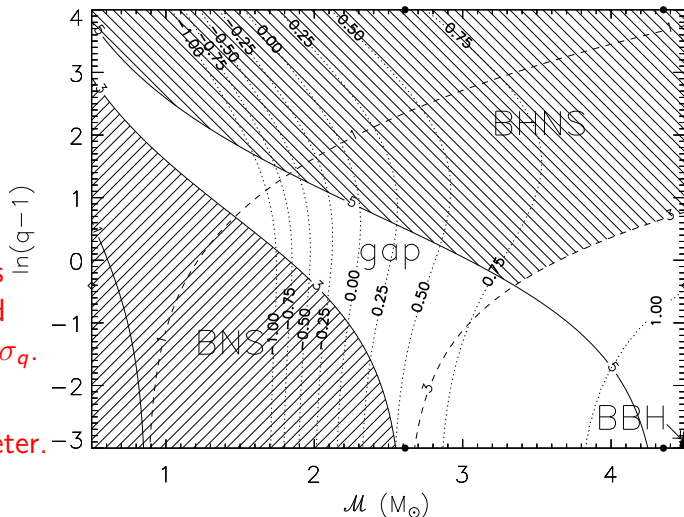
Suitable Variables

\mathcal{M} has small uncertainty $\sigma_{\mathcal{M}}$.

q has large uncertainty, but $q \in [1, \infty]$.

$\bar{q} = \ln(q - 1)$ has $\bar{q} \in [-\infty, \infty]$ and large uncertainty $\sigma_{\bar{q}}$.

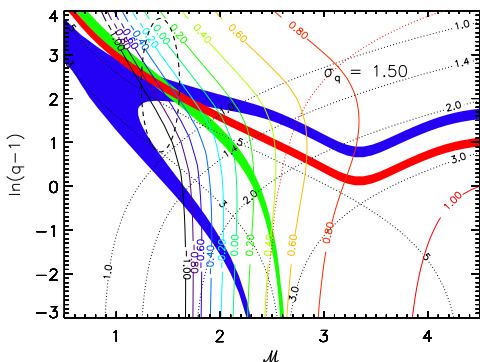
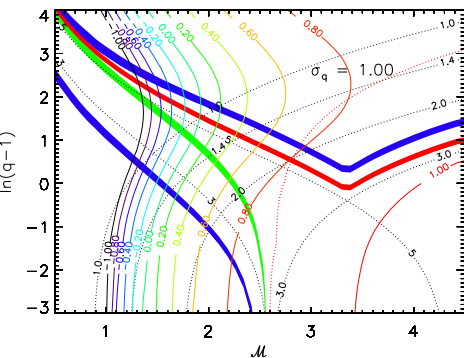
$\sigma_{\bar{q}}$ is the most important parameter.

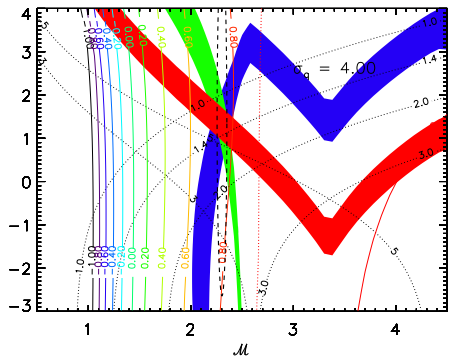
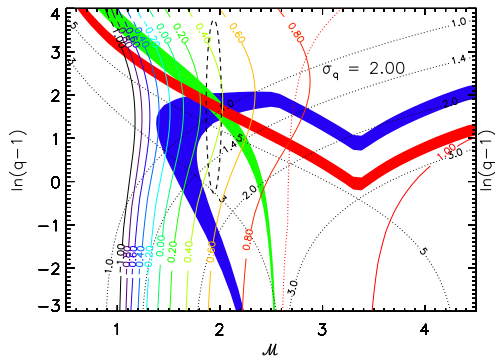


Probabilities

Assume

$$\frac{d^2 p}{d\mathcal{M}d\bar{q}} = \frac{1}{2\pi\sigma_{\mathcal{M}}\sigma_{\bar{q}}} \exp \left[-\frac{(\mathcal{M} - \mathcal{M}_0)^2}{2\sigma_{\mathcal{M}}^2} - \frac{(\bar{q} - \bar{q}_0)^2}{2\sigma_{\bar{q}}^2} \right].$$





LVC uses model of Foucart et al. (2012, 2018) to determine mass M_d remaining outside the remnant more than a few ms after a BHNS merger:

$$M_d/M_{\text{NS}}^b \simeq \alpha' \eta^{-1/3} (1 - 2\beta) - \hat{R}_{\text{ISCO}} \beta \beta' \eta^{-1} + \gamma',$$

$\beta = GM_{\text{NS}}/R_{\text{NS}}c^2$, $\eta = q(1+q)^{-2}$ and

$\hat{R}_{\text{ISCO}} = R_{\text{ISCO}}c^2/GM_{\text{BH}}$. $\alpha' \simeq 0.406$, $\beta' \simeq 0.139$, $\gamma' = 0.255$.

For the Kerr metric

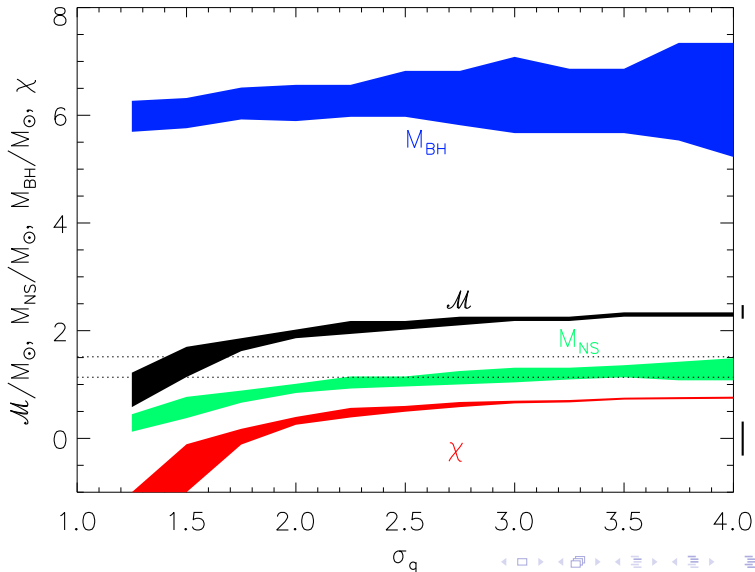
$$\chi = \sqrt{\hat{R}_{\text{ISCO}}} \left(4/3 - \sqrt{\hat{R}_{\text{ISCO}}/3 - 2/9} \right).$$

$M_d = 0$ implies

$$\hat{R}_{\text{ISCO}} = (\beta' \beta)^{-1} (\alpha' \eta^{2/3} (1 - 2\beta) + \gamma' \eta).$$

χ is found from $p_d = \int \int_{M_d \geq 0} \frac{d^2 p}{d\mathcal{M} d\bar{q}} d\mathcal{M} d\bar{q}$.

Convergence For Large σ_q

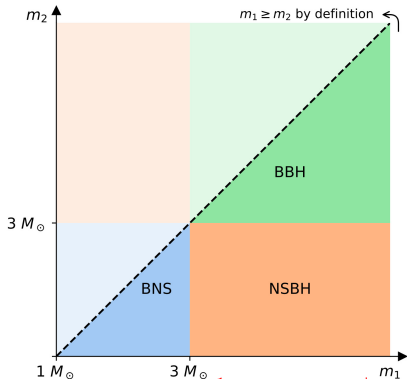


New LIGO/VIRGO/KAGRA Detections 2023

HasGap: probability that one object is between $3M_{\odot}$ and $5M_{\odot}$.

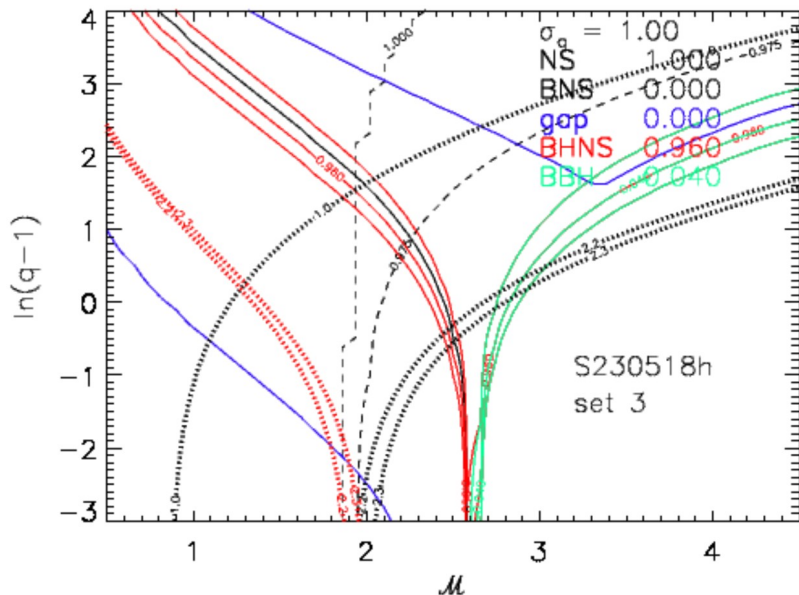
HasNS: probability that one object is between $1M_{\odot}$ and M_{max} .

rem: probability of disc formation.

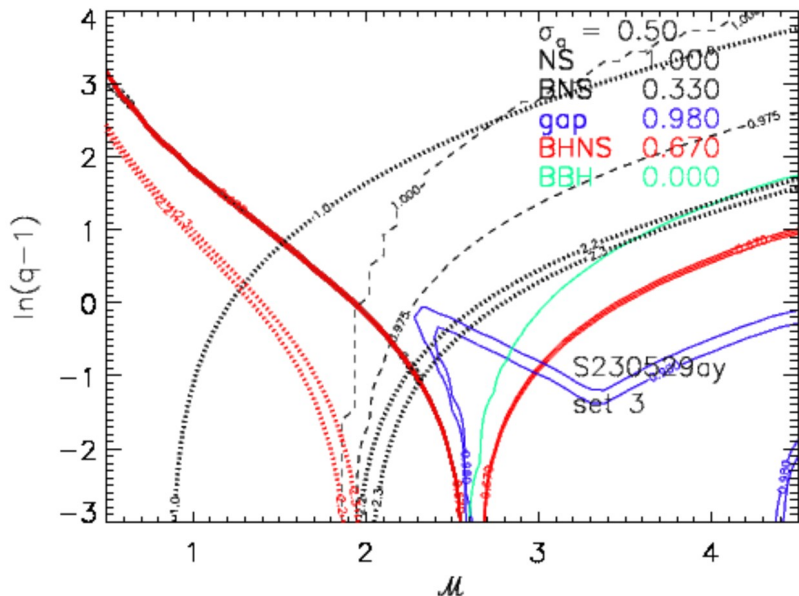


source	p_{BNS}	p_{BHNS}	p_{BBH}	p_{Gap}	p_{NS}	p_{rem}	$\text{FAR}_{\text{yr}}^{-1}$	D_{Mpc}
230518h	0.0	0.96	0.04	0.0	1.0	0.0	98	204 ± 57
230528a	0.31	0.69	0.0	0.97	1.0	0.02	9.6	261 ± 108
230529ay	0.33	0.67	0.0	0.98	1.0	0.12	160	201 ± 63
230615az	1.0	0.0	0.0	0.00	1.0	1.0	4.7	124 ± 34
230627c	0.0	0.51	0.49	0.26	0.0	0.0	100	278 ± 68

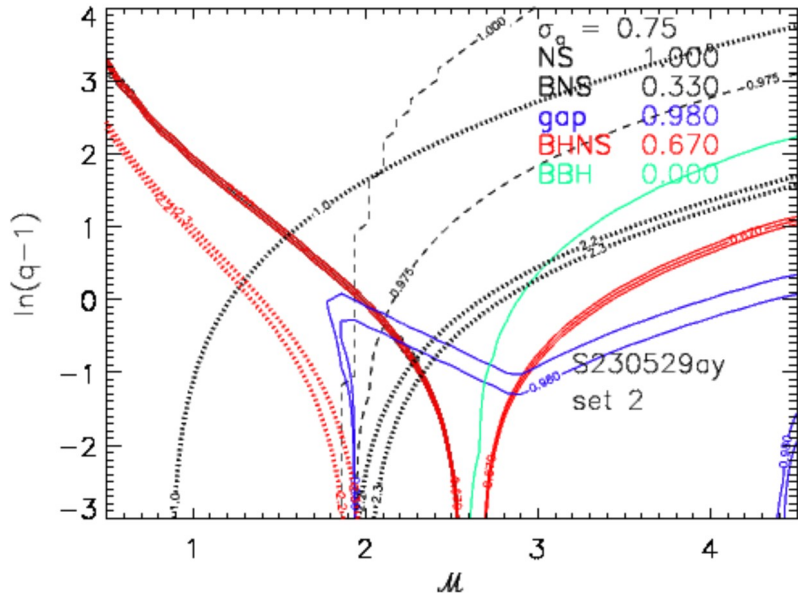
S230518h

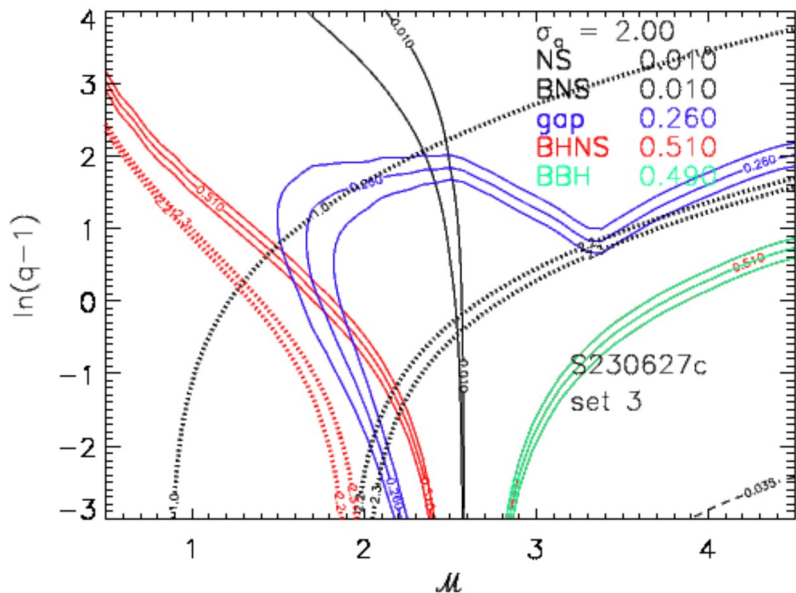


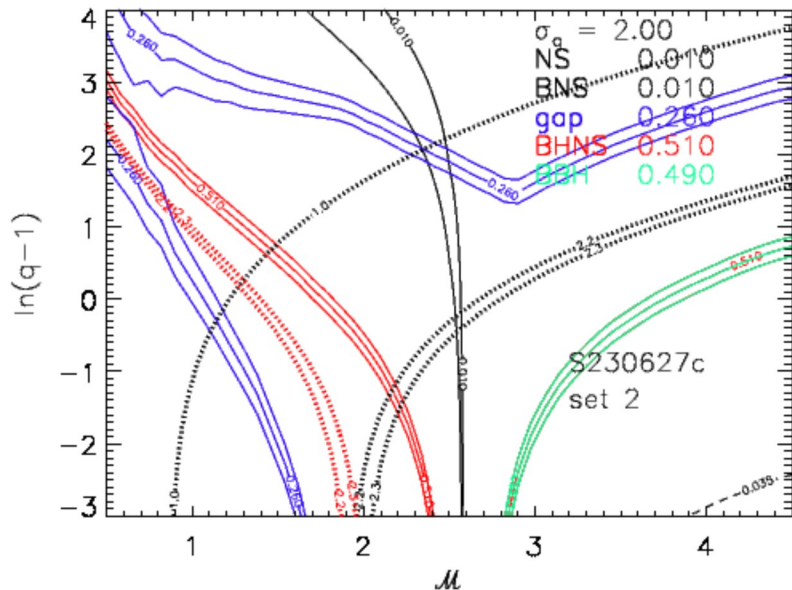
S230529ay



S230529ay







Conclusions

Nuclear experiments and theory, including EDF fits to nuclear binding energies, chiral EFT calculations, and neutron skin and dipole polarizability measurements of ^{48}Ca and ^{208}Pb , consistently predict narrow ranges for the symmetry energy parameters **without any astrophysical inputs**:

$$J = (32 \pm 2) \text{ MeV}, \quad L = (50 \pm 10) \text{ MeV}, \quad K_N = (140 \pm 70) \text{ MeV}.$$

Neutron star radius predictions are about $R_{1.4} = (11.5 \pm 1.0) \text{ km}$.

This is consistent with inferences from GW170817, NICER X-ray timing measurements and X-ray observations of quiescent thermal and photospheric radius expansion burst sources.

We eagerly anticipate new neutron skin and dipole polarizability experiments, LIGO/Virgo/Kagra observations of neutron star mergers, radio pulsar timing measurements of masses and moments of inertia measurements, and NICER and other planned X-ray telescope observations of neutron stars.